Thickness and composition of ultrathin SiO2 layers on Si

van der Marel, C; Verheijen, M.A.; Tamminga, Y; Pijnenburg, RHW; Tombros, N; Cubaynes, F

Published in:
Journal of Vacuum Science & Technology A

DOI:
10.1116/1.1701864

Publication date:
2004

Thickness and composition of ultrathin SiO_2 layers on Si

C. van der Marel, M. A. Verheijen, Y. Tamminga, R. H. W. Pijnenburg, N. Tombros, and F. Cubaynes

Citation: Journal of Vacuum Science & Technology A **22**, 1572 (2004); doi: 10.1116/1.1701864
View online: https://doi.org/10.1116/1.1701864
View Table of Contents: http://avs.scitation.org/toc/jva/22/4
Published by the American Vacuum Society

Thickness and composition of ultrathin SiO_2 layers on Si

C. van der Marel,[a] M. A. Verheijen, and Y. Tamminga
Philips Research, Eepartment Materials Analysis, Eindhoven, The Netherlands

R. H. W. Pijnenburg
Technical University Eindhoven, The Netherlands

N. Tombros
State University of Groningen, Groningen, The Netherlands

F. Cubaynes
Philips Research, Leuven, Belgium

(Received 24 October 2003; accepted 5 January 2004; published 20 July 2004)

Ultrathin SiO_2 layers are of importance for the semiconductor industry. One of the techniques that can be used to determine the chemical composition and thickness of this type of layers is x-ray photoelectron spectroscopy (XPS). As shown by Seah and Spencer [Surf. Interface Anal. **33**, 640 (2002)], it is not trivial to characterize this type of layer by means of XPS in a reliable way. We have investigated a series of ultrathin layers of SiO_2 on Si (in the range from 0.3 to 3 nm) using XPS. The samples were also analyzed by means of transmission electron microscopy (TEM), Rutherford backscattering (RBS), and ellipsometry. The thickness of the SiO_2 layers (d) was determined from the XPS results using three different approaches: the ''standard'' equation (Seah and Spencer) for d, an overlayer-substrate model calculation, and the QUASES–Tougaard [Surf. Interface Anal. **26**, 249 (1998), QUASES–Tougaard: Software package for Quantitative Analysis of Surfaces by Electron Spectroscopy, version 4.4 (2000); http://www.quases.com] method. Good agreement was obtained between the results of XPS analyses using the ''standard'' equation, the overlayer-substrate model calculation, and RBS results. The QUASES–Tougaard results were approximately 62% above the other XPS results. The optical values for the thickness were always slightly higher than the thickness according to XPS or RBS. Using the model calculation, these (relatively small) deviations from the optical results could be explained as being a consequence of surface contaminations with hydrocarbons. For a thickness above 2.5 nm, the TEM results were in good agreement with the results obtained from the other techniques (apart from QUASES–Tougaard). Below 2.5 nm, significant deviations were found between RBS, XPS, and optical data on the one hand and TEM results on the other hand; the deviations became larger as the thickness of the SiO_2 decreased. This effect may be related to interface states of oxygen, which have been investigated [D. A. Muller, T. Sorsch, S. Moccio, F. H. Baumann, K. Evans-Lutterodt, and G. Timp, Nature (London) **399**, 758 (1999); D. A. Muller and J. B. Neaton, *Structure and Energetics of the Interface Between Si and Amorphous* SiO_2 in Fundamental Aspects of Silicon Oxidation, edited by Y. J. Chabal (Springer, Berlin, 2001), pp. 219–246.] by means of high-resolution electron energy loss spectroscopy measurements of the O K edge in ultrathin gate oxides of SiO_2. © *2004 American Vacuum Society.*
[DOI: 10.1116/1.1701864]

I. INTRODUCTION

The layer system SiO_2/Si has been the subject of investigation for many years.[1–3] Photoelectron spectroscopy (XPS) is one of the techniques that have been used frequently to determine the thickness and composition of thin layers of SiO_2 on Si. In a recent set[4,5] of papers, the precise quantification of XPS analyses on thin layers of SiO_2 has been investigated in a systematic way. Much attention is paid in these papers to determine the way in which the measurements and the analysis of the results have to be carried out in order to obtain reliable results.

A comparison of various analysis techniques to determine the thickness and compositions of thin layers of SiO_2 on Si is given in Semak *et al.*[6] In this article, only layers with an optical thickness above 2 nm were investigated. For present innovations in the semiconductor industry, SiO_2 layers on Si in the range between 0.5 and 2 nm are more interesting. This motivated us to start a comparison of SiO_2/Si samples within this range, using four analysis techniques: ellipsometry, XPS, Rutherford backscattering (RBS), and transmission electron microscopy (TEM). The purpose of the work is to determine the optimal way to apply these techniques, both experimentally and with regard to the analysis of the results.

II. EXPERIMENT

The samples were based upon pure Si (100). After cleaning, a thin oxide film was grown using *in situ* steam generation oxidation. The investigated samples are given in Table I. The thickness of the SiO_2 layer ranges from 0.14 to 3.2 nm

[a]Electronic mail: cees.van.der.marel@philips.com

TABLE I. Investigated samples and thickness according to optical measurements (nine-point Woollam). The variation in the thickness across the nine measurement positions is also given.

Wafer label	Optical thickness (nm)
A	0.137±0.010
B	0.498±0.010
C	1.001±0.015
D	1.007±0.010
E	1.065±0.010
F	1.408±0.035
G	1.421±0.029
H	1.998±0.030
I	2.203±0.073
J	2.510±0.030
K	3.200±0.020
L	120

according to optical measurements. For reference purposes, measurements were also carried out on a ''thick'' SiO_2 layer on Si (120 nm, thermally grown).

All XPS analyses in this article were conducted in a Quantum 2000 of PHI. The system is operating with a monochromatic Al K_α source. Two series of XPS measurements were done. The first series of measurements was performed with a spot size of 100 μm, a pass energy of 11.75 eV, and a step size of 0.025 eV; the entrance angle of the analyzer was ±20° unless stated otherwise. A measuring angle Θ of 34° was used (Θ denotes the angle between the surface normal and the analyzer axis) and the samples were mounted such that the analyzer azimuth angle was 22.5±2° with respect to the [011] direction. By doing so, the influence of the crystal structure of the substrate upon the results is minimized.[4]

The second series of measurements was performed such, that the results could be analyzed with QUASES–Tougaard (QT).[7] Extended O 1*s* peaks (binding energy range of 430–700 eV) have been measured with a spot size of 1200×500 μm^2 (high power mode), a pass energy of 117 eV, a step size of 0.25 eV, and the analyzer entrance angle set at ±20°. Three values of the measuring angle were used: Θ=45°, 34°, and 0°.

RBS spectra were recorded with a 2 MeV He^+-ion beam, generated in a single-ended Van de Graaff accelerator. Channeling in the (100) direction was used in order to suppress the Si signal under the oxygen peak. The scattering angle used was 86.5° and the channel width was 2.165 keV. Subtraction of the silicon signal of the SiO_2 (assuming that it is stoichiometric 1:2) from the total silicon signal provided the contribution of the Si surface peak to the *total* Si peak. The Si surface peak contribution was used to normalize the integrated charge of the He^+ ions, assuming that the surface peak for elementary Si (100) corresponds to 15.5×10^{15} Si atoms/cm^2.

For the TEM analyses, perpendicular cross sections have been made by means of mechanical (tripod) polishing down to electron transparency. In order to protect the surface of the TEM sample during the preparation, a capping layer is needed. A crystalline capping layer of aluminum was used. Low-temperature vapor deposition of Al did not alter the thickness or the composition of the SiO_2 layer, as was checked by means of XPS. Aluminum is preferred as a capping layer for several reasons. The interface of polycrystalline aluminum with amorphous SiO_2 can be imaged very sharply. Glue and other amorphous materials often have a poorly distinguishable interface with oxide layers. Furthermore, aluminum has approximately the same polishing behavior as SiO_2, and is thus preferred over metals such as W or Pt that have a relatively low polishing rate. Below a W or Pt capping layer, the sample thickness at the SiO_2 layer will remain larger than the sample thickness at the underlying Si substrate; this makes accurate layer thickness measurements difficult.

The TEM analyses have been carried out in a FEI TECNAI F30 ST, operated at 300 kV. Energy-filtered TEM was applied and zero loss imaging was used as it improves the resolution by removing most of the chromatic aberrations.

III. RESULTS

First, we consider the results of the XPS measurements. A typical Si 2*p* spectrum is shown in Fig. 1(a). To determine the peak areas corresponding to elementary Si and the (sub)-oxides of Si, the Si 2*p* peaks were decomposed as follows (using the software package CasaXPS[8]). A Shirley background was subtracted. The best fit for elementary Si [Fig. 1(b)], as determined from the measurement on sample A (0.14 nm SiO_2), was obtained with two GL(67)T(1.45) curves (mixed Gauss–Lorentz with some tailing), a doublet distance of 0.61 eV and a ratio of 2:1. The decomposition into (sub)-oxides was based upon the findings of Lu and Graham:[9] doublets of GL(20) curves with a doublet distance of 0.61 eV, equal widths and at 0.97, 1.80, 2.60, and 3.9±0.2 eV distance from e-Si $2p_3$.

The first approach to determine the thickness d of the SiO_2 layer was the use of the standard equation[4]

$$d = L_{SiO_2}(E_{Si})\cos(\Theta)\ln(1 + R_{expt}/R_0), \quad (1)$$

with $L_{SiO_2}(E_{Si})$ the attenuation length for Si 2*p* electrons in SiO_2, R_{expt} the experimental ratio $I_{SiO_2}/I_{e\text{-}Si}$ and $R_0 = I^\infty_{SiO_2}/I^\infty_{e\text{-}Si}$. The parameter $I^\infty_{SiO_2}$ denotes the intensity of the Si 2*p* line of ''infinitely'' thick SiO_2, while $I^\infty_{e\text{-}Si}$ corresponds to the intensity of the Si 2*p* line of pure elementary silicon. We adopted $L_{SiO_2}(E_{Si}) = 3.448$ nm (see Seah and Spencer[4]); the measurements have been carried out for Θ=34°.

The value of R_0 is expected to depend upon the entrance angle of the analyzer. The reason is that both $I^\infty_{SiO_2}$ and $I^\infty_{e\text{-}Si}$ depends upon the entrance angle; due to the crystal effects in e-Si, the dependence of these quantities upon the entrance angle is not identical [see Fig. 5(b) in Ref. 4]. The experimental value of R_0 in our equipment has been determined by measuring a sample of pure silicon and a sample of infinitely thick SiO_2. In the spectrum of the Si 2*p* peak of sample A, no contribution of SiO_2 was detectable [see Fig. 1(b)]. Therefore, this sample was considered to be pure silicon. The experimental value of $I^\infty_{SiO_2}$ was determined using sample L.

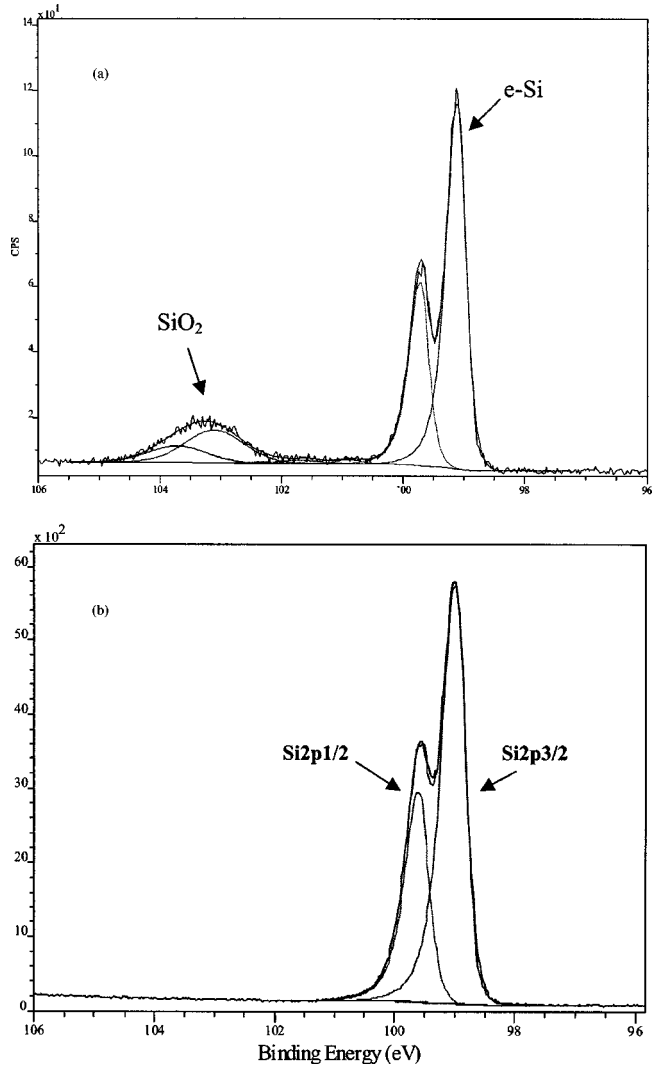

FIG. 1. (a) Typical example of a Si $2p$ peak. The spin–orbit splitting in the right-hand peak, corresponding to elementary Si, is clearly visible; the FWHM of the components of this peak is 0.31 eV. Sub-oxides are barely present between the peaks of e-Si and SiO_2. (b) Si $2p$ peak measured for the sample A ($d_{\text{optical}}=0.14$ nm); no SiO_2 contribution is visible.

The experimental values for $I^{\infty}_{SiO_2}$ and $I^{\infty}_{\text{e-Si}}$ were corrected for the attenuation of the signals due to a small amount of contamination with hydrocarbons. Combining the experimental values provides for R_0 in the Quantum 2000 at standard conditions (an entrance angle of $\pm 20°$), as follows:

$$R_0 = 0.81 \pm 0.02. \tag{2}$$

The uncertainty in the value is due to the background subtraction. Our present value nicely fits into the range of values for R_0 that is found in the literature: values between 0.6 and 0.9 have been reported. We notice that the experimental value for R_0 obtained in our equipment when a small entrance angle is used (entrance angle $\pm 4°$) is 0.91 ± 0.02. Clearly, R_0 is not a material quantity, but rather depends upon the details of the equipment. This is probably one of the reasons for the large variety of values for R_0 found in the literature.

TABLE II. Thickness in nanometers of the SiO_2 layers (d) according to the analysis of the XPS spectra with the standard Eq. (1), with QT, and with the model calculation. The thickness of the organic contamination and the total thickness (organic + SiO_2) is also given. In the right most column, the concentration ratio $[c_O/c_{Si}]$ in the SiO_2 layers, as determined in the model calculation, is shown.

	Optical thickness	Standard Eq. (1)	QT	Model calculation			
Sample	d	d	d	d	d_{org}	d_{total}	Ratio $[c_O/c_{Si}]$
A	0.14	0.0	0.11	0.04	0.28	0.32	···
B	0.50	0.29	0.73	0.36	0.16	0.53	···
E	1.07	0.56	1.20	0.66	0.19	0.85	2.8
C	1.00	0.72	1.14	0.78	0.15	0.93	2.6
D	1.01	0.77	1.35	0.83	0.18	1.01	2.5
G	1.42	1.19	1.82	1.21	0.18	1.39	2.3
F	1.41	1.21	1.92	1.24	0.14	1.38	2.4
H	2.00	1.86	2.76	1.85	0.14	1.99	2.2
I	2.20	1.94	3.10	1.92	0.09	2.02	2.2
J	2.51	2.38	3.39	2.35	0.14	2.49	2.2
K	3.20	3.09	4.71	3.03	0.11	3.14	2.1

Using the standard Eq. (1), we have calculated values for d of the series of samples. The contribution of sub-oxides was taken into account by adding a weighed average, given by

$$R_{\text{expt}} = \frac{I_{SiO_2} + 0.75 I_{Si_2O_3} + 0.5 I_{SiO} + 0.25 I_{Si_2O}}{I_{\text{e-Si}}}. \tag{3}$$

The results are given in Table II.

The XPS results were also analyzed using a model calculation, in which the samples are assumed to consist of a substrate of pure Si, a SiO_2 layer with thickness d, and an organic contamination containing only the elements C and H, with thickness d_{org}. The principle of this method is presented only briefly; for details and other examples of applications, we refer to Ref. 10. Within the model, simple exponential attenuation of the XPS signals is assumed. The intensity of the C $1s$ signal is expressed in terms of the thickness d_{org}, the atomic density of the organic contamination, the XPS cross section or the sensitivity factor of the C $1s$ line, the attenuation length $L_C(\text{C}\,1s)$ for C $1s$ electrons in the organic top layer, and a number of instrumental parameters, such as the x-ray flux, the transmission function, the detector efficiency for a given kinetic energy E_i, and the correction factor for the asymmetry effect. Similar expressions can be derived for the intensity of the O $1s$ signal, the intensity of the Si $2p$ signal originating in the SiO_2 layer, and the Si $2p$ signal coming from the e-Si substrate. For the attenuation in the organic contamination, we adopted values for the IMFP given by Cumpson.[11] Elastic scattering in the SiO_2 layer and in the substrate was taken into account by using values for the attenuation length, taken from Ref. 4. This provides, all together, four equations with four unknown parameters: the thickness of the organic contamination d_{org}, the thickness of the SiO_2 layer d, the concentration ratio $[c_O/c_{Si}]$ in the SiO_2 layer, and the x-ray flux. Reversal of these equations provides expressions for d, d_{org}, and $[c_O/c_{Si}]$ in terms of the

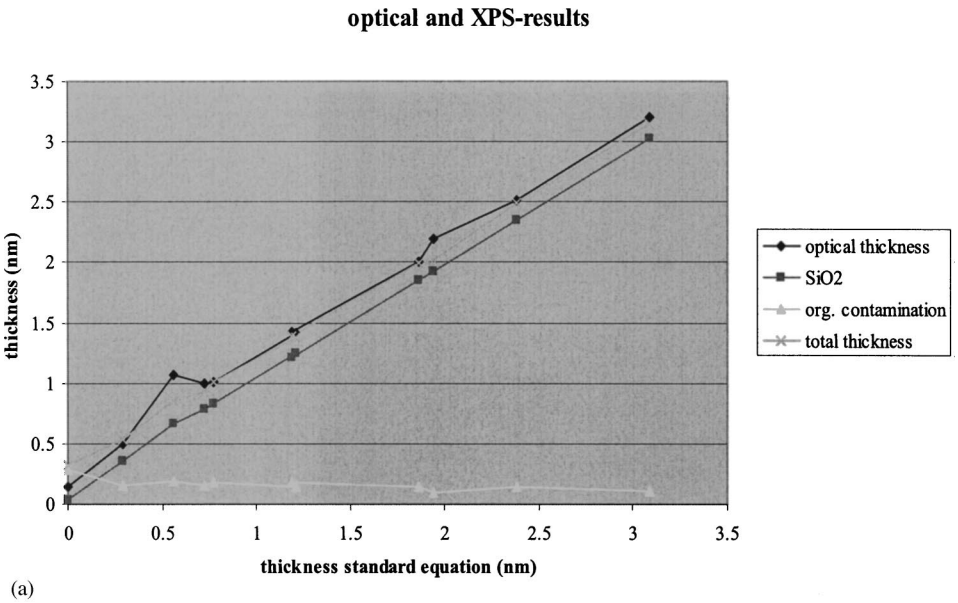

(a)

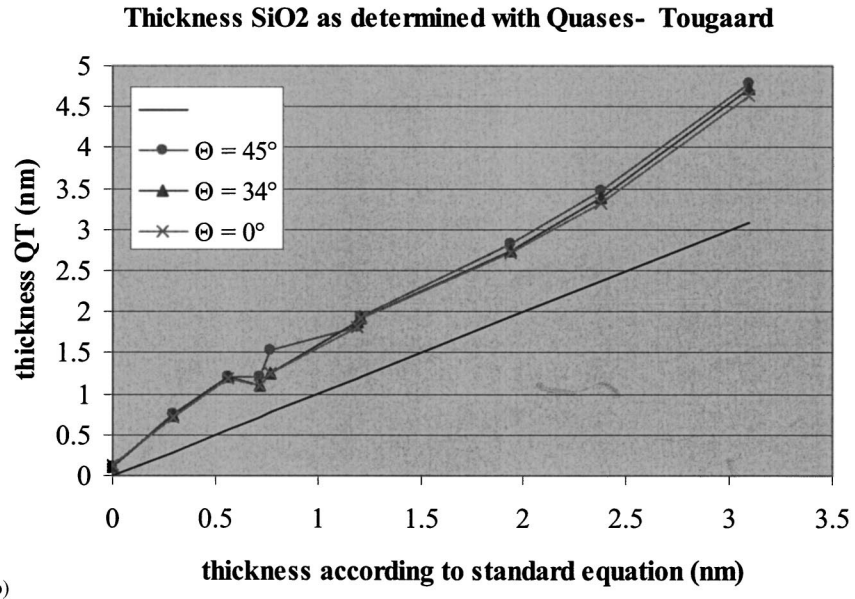

(b)

FIG. 2. Thickness of the SiO_2 layers obtained with various methods, plotted as a function of the thickness according to the standard Eq. (1). (a) Optical data and results of the model analysis. (b) Results of the analysis of extended O 1*s* peaks with QT for $\Theta=0°$, 34°, and 45°.

measured intensities. This model analysis has been applied to the present set of XPS analyses, all for $\Theta=34°$ and azimuth $=22.5°$. The sensitivity factor for the Si 2*p* peak was chosen such that for sample L (not-contaminated, infinitely thick SiO_2), the ratio $[c_O/c_{Si}]=2.0$ was obtained. The intensity of the Si 2*p* peak of elementary signal depends—due to crystal effects—upon the measuring geometry (Θ and azimuth), and is also reduced by intrinsic plasmon losses.[12] To take these effects into account, the measured signal of the Si substrate was divided by $R_0^{th}/R_0^{exp}=0.65$ with $R_0^{th}=0.529$ (see Ref. 4) and $R_0^{exp}=0.81$ [Eq. (2)]. The results of the analysis are given in Table II and in Fig. 2(a).

The thickness of SiO_2 layers on Si can also be determined by means of an analysis of the e-loss phenomena of the O 1*s* peak, using the method called QUASES–Tougaard.[7] An interesting property of this method is that it is *independent of crystal effects*, because the amount of oxygen is being determined. Measurements of the extended O 1*s* peaks have been carried out for $\Theta=0°$, 34°, and 45°. Extended SiO_2 peaks of sample L were used as a reference (to "scale" the spectra[7]); for the attenuation length of O 1*s* electrons in SiO_2, we adopted the value $L_{SiO_2}(E_{O\,1s})=2.551\,nm$[1]. The results of the QT analysis obtained at different angles are in very good mutual agreement, the differences being <0.2 nm [see Fig. 2(b)]. Average values of the thickness of the SiO_2 layers are given in Table II.

Next, we consider the results of the RBS measurements. The simulation program RUMP was used to model the spectra and to determine the amount of oxygen at the surface. During RBS analysis, some carbon deposition occurs at the surface of the samples due to cracking of hydrocarbons in the

TABLE III. Amount of oxygen at the surface according to the RBS measurements and thickness of the SiO_2 layers (d) according to RBS, TEM, and the XPS model calculation (d in nm).

Sample	Optical d	RBS O atoms $[10^{15}/cm^2]$	RBS d	TEM d	XPS model calculation d
A	0.14	1.12	0.03		0.04
B	0.50	2.4	0.31		0.36
D	1.01	5	0.88	1.37	0.83
E	1.07	4.7	0.81		0.66
F	1.41	7.62	1.45	1.68	1.24
G	2.00	10.1	2.00	2.12	1.85
J	2.51	12.5	2.53	2.43	2.35
K	3.20	16	3.29	3.33	3.03

vacuum of the RBS instrument, as a consequence of the irradiation with high-energy He ions. In parallel to the deposition of carbon, we observed an increase of the amount of oxygen at the surface by 1.0×10^{15} O atoms/cm^2. The amount of oxygen was found to be independent of the irradiation time. Probably the oxygen is due to adsorbed water, which is ''buried'' below the carbon layer. This hypothesis was confirmed by XPS analysis of a number of samples both before and after the RBS analysis. The raw RBS data were corrected for the influence of the ''buried'' oxygen (1.0×10^{15} atoms O/cm^2 was subtracted). The thickness of the SiO_2 layers was obtained using a density of 2.27 g/cm^3, corresponding to an atomic density of 6.83×10^{22} atoms/cm^3. The results of the layer thickness measurements with RBS are shown in Table III.

Finally, we consider the TEM analyses. A typical TEM photograph is shown in Fig. 3. For each sample, at least three high-resolution images were stored that were taken from areas at least a few micrometers apart. The magnification was calibrated on every image studied; the calibration factor that was determined for each image appeared to be nearly constant for all images studied, illustrating the intrinsic reproducibility of the instrument. The thickness was determined using a box, drawn with its edges parallel and perpendicular to the surface normal. Within this box, two parallel lines are drawn that are manually aligned to the SiO_2/Si and SiO_2/Al interfaces. The thickness determined for the various samples determined in this way is given in Table III. Changing the site of the interface (i.e., *on* a row of atoms or *between* two rows of atoms) results in a 0.10 to 0.15 nm shift in the resulting thickness values. This is the main source for errors. Consequently, we estimate the absolute accuracy of the TEM thickness values in Table III to be ±0.1 nm.

IV. DISCUSSION

First, we consider the results in Table II. The thickness of the SiO_2 layers according to the model calculation is always less than the optical thickness, the difference being, on average, 0.2 ± 0.1 nm. It is interesting to see that the ''total thickness'' ($d+d_{org}$) is in good agreement with the optical thickness. Apparently, the optical measurements determine the

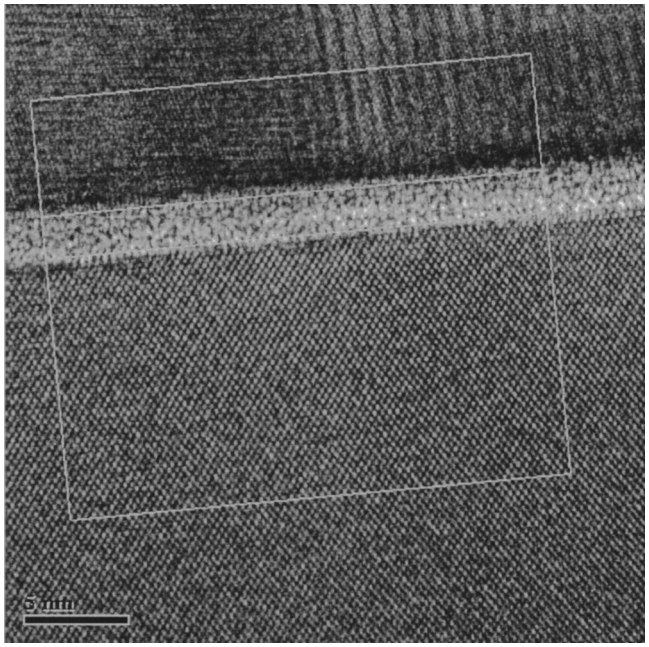

FIG. 3. TEM photograph of sample G. The upper layer in the photograph shows the aluminum capping layer. The layer below the aluminum layer is the SiO_2 layer. The box in the picture is used to determine the thickness d of the SiO_2 layer. The lattice distance of the elementary silicon was used for the calibration of the TEM photographs.

thickness of the *combination* of SiO_2 layer and the organic contamination. The thickness obtained with the standard Eq. (1) is in good agreement with the results of the model analysis: the difference is, on average, 0.02 nm, the largest difference being 0.10 nm.

The concentration ratio $[c_O/c_{Si}]$ in the layers is within the experimental accuracy close to 2.0 for $d>2.5$ nm, but increases when the thickness decreases. For thin SiO_2 layers (≈1 nm), the precision is typically ±0.2 as a consequence of the statistical errors in the curve fit results; the precision is better for thicker SiO_2 layers. The deviating values of $[c_O/c_{Si}]$ are not due to an oxygen component in the organic contamination, as the C 1*s* peak in all cases corresponded to a aliphatic hydrocarbon without a detectable fraction of C–O bonds, and because the thickness of the organic contamination was always less than 0.2 nm. This point is discussed further in Ref. 10.

The results of the QT approach were, in all cases, above the results according to the standard equation, the model calculations, and the optical thickness; the difference between the QT results and the standard equation is, on average, 62% for $d_{opt}\geqslant1$ nm.

The RBS results were, after a correction for the adhesion of oxygen during the RBS measurements, in good agreement with the results of the standard equation and the model calculation, the difference being, on average, less than 0.1 nm (see Table III). We also notice that, in previous analyses, differences have been found between the results according to QT and RBS results of, on average, 45% (see Ref. 6, Table 5). Apparently, the modeling that is being used in the software package QT is not completely accurate for SiO_2.

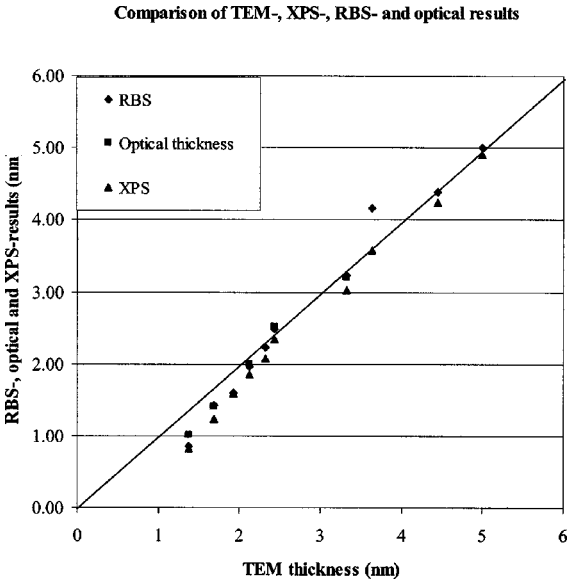

FIG. 4. Thickness of the SiO_2 layer according to RBS, XPS, and optical analysis, plotted as a function of the thickness according to TEM measurements. The data points corresponding to TEM thicknesses of 1.9, 2.3, 3.8, 4.4, and 5.0 nm were obtained as part of our CCQM-P38 measurements (see Ref. 13).

Finally, we consider the TEM results. In Fig. 4, the thickness of the SiO_2 layers according to the XPS, RBS, and optical measurements have been plotted as a function of the thickness according to TEM. Recently, an interlaboratory comparison of TEM, RBS, and XPS analyses has been done within the framework of the CCQM-P38 project.[13] The results on the thin SiO_2 samples that were obtained in our laboratory are also included in Fig. 4. These results are consistent with the present set of data.

For layers with a thickness *above* 2.5 nm, the results are in agreement within the experimental accuracies. Yet, for layers with a thickness *below* 2.5 nm, the TEM values are significantly larger than the other values (optical, XPS, RBS). The deviation might tentatively be explained by assuming that the density of these ultrathin SiO_2 layers is less than the density of bulk SiO_2. This will clearly influence the thickness as determined by RBS; in addition, the attenuation lengths in XPS are expected to increase when the density of a material decreases. Yet, as can be seen in Table III, the deviation for sample D is nearly 40%, and it seems unlikely that the density of SiO_2 in these layers is 40% less than the density of bulk SiO_2. A different tentative explanation is as follows. According to Muller *et al.*[14,15] the electron energy loss spectroscopy (EELS) spectrum of the oxygen atoms at the SiO_2/Si interface is different from that of bulk SiO_2, indicating that the chemical environment of the oxygen atoms at the interface is different from bulk SiO_2. Further, the thickness of the SiO_2 layer that is obtained by measuring the O *K* edge as a function of position across the SiO_2 layer is significantly larger than the optical thickness (see Fig. 3 in Ref. 14, where it was shown that the *optical thickness* is 1 nm, whereas the *total* O *signal* has a full width at half-maximum (FWHM) of 1.6 nm). The results suggest that some of the surface oxygen atoms "penetrate" into the e-Si; this may give rise to a seemingly thicker SiO_2 layer in TEM images, as electron energy loss effects influence the intensity of the transmitted beam. This conjecture is corroborated by recent high-resolution TEM analyses of SiO_2/Si interfaces by Ikarashi *et al.*[16] Nanometer-scale SiO_2 protrusions have been found, one or two atomic layers in size, randomly formed beneath the amorphous SiO_2 layer. For a sample in which the optical thickness of the SiO_2 is 1.8 nm, the FWHM of the total O signal is 2.1 nm.[14,15] Apparently, the penetration of interfacial oxygen into the silicon decreases as a function of increasing thickness of the SiO_2 layer. This may explain the disappearance of the discrepancy between TEM thickness and XPS or RBS thickness as a function of increasing SiO_2 thickness. Yet, the reason that the penetration effect at the SiO_2/Si interface depends upon the thickness of the oxide layer for $d<2.5$ nm remains unknown.

V. CONCLUSIONS

We have shown that the determination of the thickness of ultrathin SiO_2 layers using RBS, using the standard equation for XPS, or applying a model analysis of XPS results provides consistent results. Model analysis of XPS results demonstrated in a quantitative way that deviations from the optical results are a consequence of surface contaminations of the samples with hydrocarbons. QUASES–Tougaard analysis of extended O 1*s* peaks has also been applied. The results were found to be independent of crystal effects, as expected. Yet, the thickness of the SiO_2 layers was approximately 62% higher than the thickness determined with the other methods.

TEM results are in agreement for thickness exceeding 2.5 nm, but in samples with SiO_2 layers <2.5 nm, the TEM thickness is larger than the RBS or XPS thickness. Together with this effect, we have observed that the concentration ratio $[c_O/c_{Si}]$ in these layers is larger than 2.0 and increases when the SiO_2 thickness decreases. The effects may be related to penetration of interfacial oxygen into silicon, as observed using EELS in ultrathin gate oxides of SiO_2 and visible as protrusions of SiO_2 into silicon in high-resolution TEM images.

[1]J. M. Hill, D. G. Royce, C. S. Fadley, L. F. Wagner, and F. J. Grünthaner, Chem. Phys. Lett. **44**, 225 (1976).
[2]F. J. Himpsel, F. R. McFeely, A. Taleb-Ibrahimi, J. A. Yarmoff, and G. Hollinger, Phys. Rev. B **38**, 6084 (1988).
[3]Z. H. Lu, J. P. McCaffrey, B. Brar, G. D. Wilk, R. M. Wallace, L. C. Feldman, and S. P. Tay, Appl. Phys. Lett. **71**, 2764 (1997).
[4]M. P. Seah and S. J. Spencer, Surf. Interface Anal. **33**, 640 (2002).
[5]M. P. Seah and S. J. Spencer, J. Vac. Sci. Technol. A **21**, 345 (2003).
[6]B. S. Semak, C. van der Marel, and S. Tougaard, Surf. Interface Anal. **33**, 238 (2002).
[7]S. Tougaard, Surf. Interface Anal. **26**, 249 (1998); S. Tougaard, QUASES–Tougaard: Software package for Quantitative Analysis of Surfaces by Electron Spectroscopy, version 4.4 (2000); http://www.quases.com
[8]Software package for the analysis of XPS results, CasaXPS version 2.2.32, see http://www.casaxps.com
[9]Z. H. Lu, M. J. Graham, D. T. Jiang, and K. H. Tan, Appl. Phys. Lett. **63**, 2941 (1993).
[10]C. van der Marel, M. Yildirim, H. Gruell, and H. R. Stapert, J. Vac. Sci. Technol. A (in preparation).
[11]P. J. Cumpson, Surf. Interface Anal. **31**, 23 (2001).

[12]T. Katayama, H. Yamamoto, M. Ikeno, Y. Mashiko, S. Kawazu, and M. Umeno, Jpn. J. Appl. Phys. **38**, 4172 (1999).
[13]M. Seah, J. Vac. Sci. Technol. A, these proceedings.
[14]D. A. Muller, T. Sorsch, S. Moccio, F. H. Baumann, K. Evans-Lutterodt, and G. Timp, Nature (London) **399**, 758 (1999).
[15]D. A. Muller and J. B. Neaton, *Structure and Energetics of the Interface Between Si and Amorphous SiO_2* in Fundamental Aspects of Silicon Oxidation, edited by Y. J. Chabal (Springer, Berlin, 2001), pp. 219–246.
[16]N. Ikarashi, K. Watanabe, and Y. Miyamoto, J. Vac. Sci. Technol. A **21**, 495 (2003).